Electron-probe micro-analysis of the iron–titanium oxides in some New Zealand ironsands

By J. B. Wright

Geology Department, Otago University, New Zealand

and J. F. Lovering

Geophysics Department, Australian National University, Canberra

[Taken as read 4 November 1965]

Summary. The electron probe was used to analyse for Fe, Ti, Mg, Al, and Mn. Vanadium could not be determined because of interference from Ti. Calcium was shown to be present only in inclusions of apatite and silicate; it does not occur in the titanomagnetite structure.

Homogeneous grains (magnetite–ulvöspinel solid solutions) do not vary greatly in bulk composition, averaging close to 61 % Fe and 8 % TiO_2. Inhomogeneous grains contain variable amounts of hematite–ilmenite lamellae produced by progressive oxidation of the homogeneous grains. In the early stages there is rapid build-up of titanium in the rhombohedral lamellae, which are initially relatively poor in iron. As oxidation proceeds the almost titanium-free cubic phase becomes strongly enriched in magnesium, aluminium, and manganese, while the iron: titanium ratio in the rhombohedral phase increases. The end-product may be a homogeneous titanhematite, if initial concentrations of Mg, Al, and Mn are low. Otherwise residuals of a relatively iron-poor almost titanium-free (Mg, Al, Mn)-enriched cubic phase remain in the titanhematite. The behaviour of iron and titanium agrees with recent synthetic work in the system. Some of the oxidized grains contain transparent spinel lamellae exsolved from the cubic phase. Exsolution may commence at different stages in the oxidation process, but the reason is not clear—there are no significant differences in the composition of phases with and without spinel lamellae.

Analyses and normative compositions are presented for the different phases in each grain, where possible. The compositional changes accompanying oxidation satisfactorily explain the slope of the thermomagnetic curves: there is no need to invoke bulk compositional variations within a given ironsand sample.

Samples from an ilmenite and a non-titaniferous magnetite concentrate were also briefly examined.

MAGNETIC concentrates of ironsands from the North Island of New Zealand are, mostly, homogeneous magnetite–ulvöspinel solid solutions. A small proportion of inhomogeneous grains contains hematite–ilmenite intergrowths and, less commonly, exsolved aluminous spinel lamellae. Such grains develop by progressive oxidation of homo-

geneous magnetite–ulvöspinel solid solutions with homogeneous titanhematite as the ideal end product (Wright, 1964, 1965; cf. Buddington and Lindsley, 1964).

The electron-probe X-ray micro-analyser has been used in the study of these ironsands to determine: the chemical homogeneity within and between the homogeneous grains; also the elemental distribution between the host phase and segregated hematite–ilmenite and aluminous spinel phases in inhomogeneous grains, as a function of progressive oxidation of original homogeneous grains.

Analytical method. The electron-probe X-ray microanalyser is now well established as a valuable tool in mineralogical and petrological studies (e.g. Lovering and White, 1964). In the present study an Applied Research Laboratories instrument was used to determine Fe, Ti, Mn, Al, Mg concentrations in the samples. Calcium has also been reported as a minor constituent in the ironsands (Wright, 1964) but some workers (e.g. Vincent *et al.*, 1957) have pointed out that Ca is unlikely to enter into the titanomagnetite structure and that its invariable but varying appearance in analyses is due to calcium-bearing inclusions in the samples. Much of the calcium in the ironsand analyses reported by Wright (1964) is due to apatite inclusions (fig. 1) but calcium-bearing silicate inclusions are probably also present. Vanadium concentrations of 0·36 to 0·47 % V_2O_3 have been reported in these ironsands (e.g. Wright, 1964), but vanadium analyses were not possible with the analytical methods available, since the V-$K\alpha$ radiation (2·505 Å) was interfered with by the Ti-$K\beta$ radiation (β_1 = 2·514 Å, β_2 = 2·498 Å).

All analyses were carried out using an accelerating potential of 10 KV on the primary electron beam (minimum width approximately 1 μ but sometimes 2–3 μ). In general, two separate series of analyses were carried out to make full use of the three separate spectrometers on the instrument. In the first series Fe, Mn, and Mg were determined together and in the second series Ti and Al. All X-ray intensities were corrected for beam-current drift, detector dead-time, and background. Mass absorption corrections were made using data given by Birks (1963). Final correction factors were derived for each element analysed by using a selection of standard phases (pure metals, titanium-free magnetite, magnesian ilmenite, magnesian spinel, sapphire). As far as accuracy of the measurements is concerned, comparison with chemical analyses (table I below) shows that they cannot be seriously in error.

Results

Homogeneous titanomagnetite grains. Analyses were made along short step traverses of up to 10 μ interval, or on random spots, to test for compositional inhomogeneities within individual grains, of which no evidence was found.

Four full and two partial analyses are given in table I, together with a simplified average chemical analysis, calculated from Wright, 1964, table 4, and recast as a homogeneous titanomagnetite.

The somewhat arbitrary norms are believed to be the simplest way of deriving a measure of the oxygen balance in the analysis and apportioning it between Fe^{2+} and Fe^{3+}. They indicate the variation in amount of

different potential phases present, particularly for inhomogeneous grains, which will be discussed presently. Limiting Fe_3O_4 contents are calculated by assuming that all the Fe_2O_3 is combined with FeO as magnetite (cf. Vincent *et al.*, 1957).

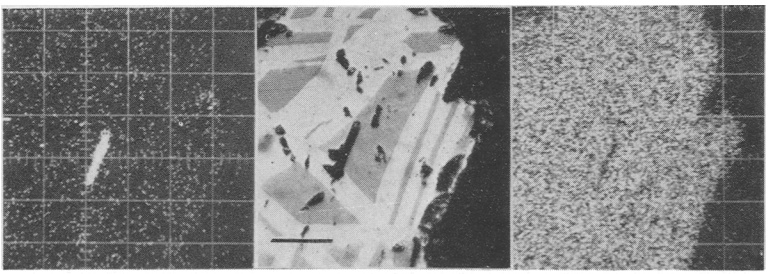

FIG. 1. X-ray scan pictures, 10 KV excitation potential, to show localization of calcium in apatite inclusion in titanomagnetite grain (titanomagnetite concentrate, Waikato North Head. No. 4, also fig. 5 of Wright, 1964). Scale bar represents 20μ.

Inhomogeneous grains. There are two main types: Grains with varying amounts of a hematite–ilmenite phase formed by oxidation of original homogeneous magnetite–ulvöspinel solid solutions; three grains were partly analysed and five grains fully analysed, including one completely oxidized to homogeneous titanhematite. And grains with the hematite–ilmenite phase as above, and exsolved aluminous spinel lamellae; one grain was partly and two grains fully analysed; the aluminous spinels were exsolved on so fine a scale that only partial resolution was possible with the electron beam.

Most analyses were made along 2μ step traverses across selected portions of each grain. The results are summarized on succeeding pages as profiles showing weight per cent. of each element plotted against traverse distance. Traverse vectors are indicated on the accompanying photomicrographs. For some grains data from adjacent traverses could be combined into composite profiles. All fully analysed grains and one partially analysed grain are figured. The remainder merely provide confirmatory information.

Compositions and normative recalculations for the major phases in each grain are also presented (table II). Where profiles are of simple aspect (e.g. fig. 3, grain no. 8) there is no problem in such recalculations. Where profiles are uneven and provide different data for traverses over

TABLE I. Analyses of homogeneous titanomagnetite grains

	1	2	3	4	5	6	Average chemical analysis
Fe	60·5	60·9	60·6	58·4*	61·6	n.d.	60·6
Mg	2·1	2·0	2·6	2·5	n.d.	n.d.	1·9
Mn	0·2	0·3	0·3	0·3	n.d.	n.d.	0·5
Ti	3·9	4·6	6·0	4·3	n.d.	5·4	4·7
Al	3·5	2·1	1·9	2·7	1·0	1·7	1·7
Potential normative composition (wt %)							
$MgAl_2O_4$	9·2	5·5	5·0	7·1	—	—	4·5
$MgFe_2O_4$	4·6	8·8	14·6	10·6	—	—	9·6
$MnFe_2O_4$	0·9	1·4	1·4	1·4	—	—	1·8
Fe_3O_4	66·8	63·1	52·2	57·5	—	—	59·9
Fe_2TiO_4	18·1	21·5	28·0	20·2	—	—	22·0
	99·6	98·9	101·2	96·8	—	—	98·0
Limiting wt % Fe_3O_4	73	73	71	71			73

Nos. 1, 2, 3, and 5 from titanomagnetite concentrate, Raglan (no. 3 of Wright, 1964).

Nos. 4 and 6 from titanomagnetite concentrate, Waikato North Head (no. 4 of Wright, 1964).

* Low Fe value attributed to unusually short traverse very close to silicate inclusion.

different parts of the same phase (e.g. fig. 2, grain no. 7) subjective selection of amounts to incorporate into these norms was sometimes necessary, in order that the totals might approach 100 %. Compositional inhomogeneities apart, such irregularities in profiles could be due to electron penetration of a near-surface boundary between the segregated phases or between the analysed phase and an inclusion. For most grains, the former is more likely, in which case compositional differences between coexistent phases can be regarded as minima. Interference between the major iron–titanium oxide phases would reduce figures for Fe, Mg, Mn, and Al in cubic phases and increase them in the rhombohedral portions, and vice versa for Ti.

Relative proportions of magnetite–ulvöspinel and hematite–ilmenite phases were estimated by cutting up and weighing photomicrographs. For the random sections the photographs must be assumed to represent, such a procedure will give a measure of relative volumes. Since the specific gravities of the two phases are probably very close, the relative volumes will also be a measure of their relative proportions by weight.

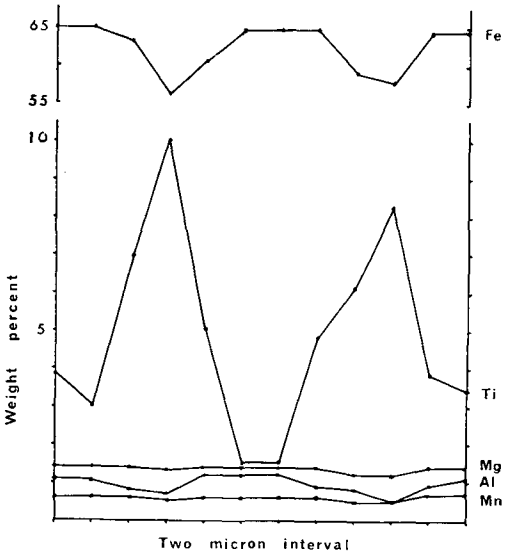

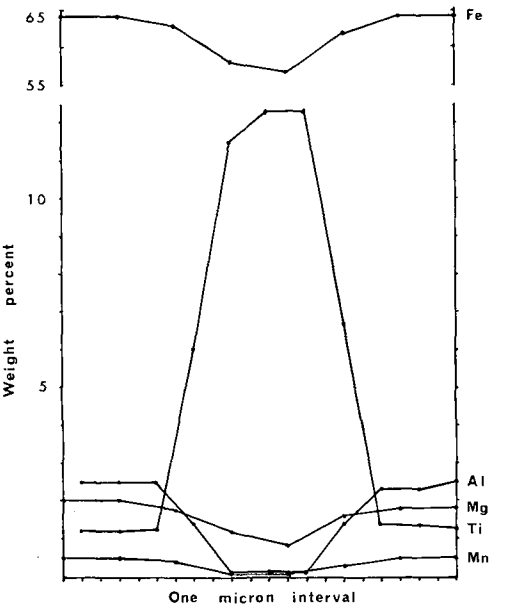

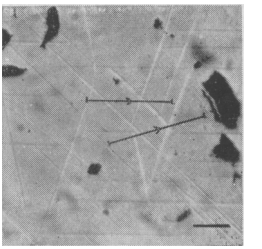

FIGS. 2 and 3: FIG. 2 (top). Grain no. 7 (in titanomagnetite concentrate, Raglan. No. 3 of Wright, 1964). Lower traverse on photomicrograph (2μ steps): Fe, Mg, Mn. Upper traverse on photomicrograph (2μ steps): Ti, Al. Scale bar represents 10μ. *Note.* Coincidence of profile peaks from the two traverses is purely fortuitous.

FIG. 3 (bottom). Grain no. 8 (in titanomagnetite concentrate, Raglan. No. 3, also fig. 6 of Wright, 1964). Upper traverse on photomicrograph (3μ steps): Fe, Mg, Mn. Lower traverse on photomicrograph (2μ steps): Ti, Al. Scale bar represents 10μ. *Note.* The faint cloudiness in the cubic phase in lower right is extremely fine-scale transparent spinel exsolution.

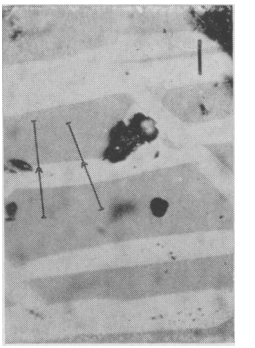

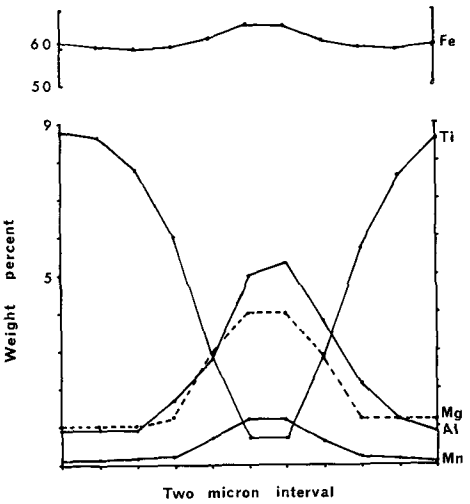

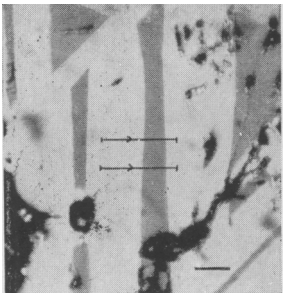

FIGS. 4 and 5: FIG. 4 (top). Grain no. 9 (in titanomagnetite concentrate, Waikato North Head. No. 4 of Wright, 1964). Upper traverse on photomicrograph (2μ steps): Fe, Mg, Mn. Lower traverse on photomicrograph (2μ steps): Ti, Al. Scale bar represents 10μ. *Note.* Sparse transparent spinel lamellae visible in the cubic phase, extreme upper left.

FIG. 5 (bottom). Grain no. 11 (in titanomagnetite concentrate, Raglan. No. 3 of Wright, 1964). Upper traverse on photomicrograph (2μ steps): Fe, Mg, Mn. Lower traverse on photomicrograph (2μ steps): Ti, Al. Scale bar represents 10μ. *Notes.* The Rhombohedral phase is darker than the host titanomagnetite and must therefore be close to pure $FeTiO_3$ (see text). The sympathetic variation of Ti and Al profiles is attributed to very fine-scale spinel exsolution bordering the narrow ilmenite lamellae and visible only at extreme magnification. Neither phase was fully resolved by the electron beam, so composition figures are simply average values from each traverse.

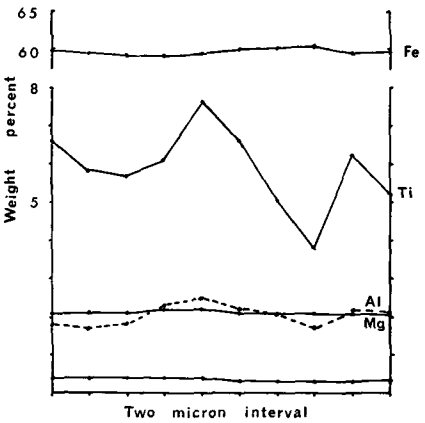

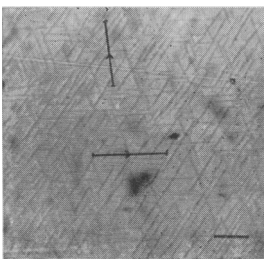

From these figures, possible bulk compositions have been calculated (table II) for comparison with those of homogeneous grains in table I. X-ray scanning pictures for two grains are also appended, to supplement the profiles.

Discussion

Major constituents. Fig. 11 summarizes molecular compositions for all fully analysed grains in terms of (limiting Fe_3O_4)/(substituted ulvöspinel) for cubic phases, and Fe_2O_3/(substituted ilmenite) for rhombohedral phases. Tie-lines join the compositions of coexisting phases.

Grains in advanced stages of oxidation (e.g. no. 9) are likely to be at or near equilibrium because by this stage virtually all the titanium is in the rhombohedral phase and little further migration of major constituent cations is involved—the main change on further oxidation is conversion of Fe^{2+} to Fe^{3+}. (Titanhematite grains with cubic phases very rich in aluminous spinel constituents (e.g. no. 10) have irregular profiles, however, and cannot be near equilibrium.) Except in the least oxidized grains, all rhombohedral phases coexist with a very titanium-poor magnetite phase. This is consistent with the data summarized in fig. 5 of Buddington and Lindsley (1964), where the gap in experimental data for equilibrium compositions ($magnetite_{90}ulvöspinel_{10}$ to $magnetite_{100}$ and $hematite_{15}ilmenite_{85}$ to $hematite_{100}$) shows that great increases in Fe_2O_3 content of the rhombohedral phases can be accompanied by only small changes in composition of coexisting equilibrium cubic phases.

At earlier stages in the oxidation process equilibrium rhombohedral phases must be close to $FeTiO_3$. Much titanium would have to migrate over comparatively long distances to become concentrated in a few narrow lamellae, if equilibrium were to be attained. Failure to reach such equilibrium could be one reason for the low Ti values in rhombohedral phases of weakly oxidized grains such as no. 7 and for some irregularity in their profiles. A more likely explanation is that the lamellae are too narrow (1μ wide) to have been completely resolved by the 2μ step traverses of the electron beam. The low Ti figure in the calculated bulk composition is consistent with this hypothesis, particularly as the lamellae retain a very faint pink tinge in oil and are slightly pleochroic. Vincent *et al.* (1957) have shown that ilmenite of this appearance may contain as little as 10 % Fe_2O_3. Compare grain no. 11, in which rhombohedral lamellae are greyer than the host and

TABLE II. Analyses of composite grains (figs. 2 to 10), and of a homogeneous titanhematite grain (no. 14), with norms and estimated approximate bulk composition. C, cubic phase; R, rhombohedral phase; C_1 and C_2, cubic phases 1 and 2 of grain 12; Av., average

Grain	7		8		9		10		12†			13	11	14§
Figure	2		3		4		6 & 7		8 & 9			10	5	—
	C	R	C	R	C	R	C	R	C_1	C_2	R	—	Av.	R
Fe	65·0	56·5	64·2	55·2	58·0	56·6	45·8	60·0	63·1	55·6	52·5	—	59·4	59·6
Mg	1·4	0·2	2·0	0·8	4·0	1·0	8·7	1·5	3·5	4·1	2·0	—	2·1	1·0
Mn	0·6	2·5	0·5	0·1	1·2	0·1	0·3	0·3	0·5	0·3	0·2	—	0·4	0·3
Ti	2·5	10·0	1·2	12·3	0·7	8·8	0·3	6·0	0·7	—	12·5	—	5·7	4·9
Al	1·1	0·5	2·5	0·1	5·3	0·9	8·3	0·7	2·5	10·4	0·6	—	2·0	1·4
Limiting wt % Fe_3O_4	85		88		71		27		72			—	68	—
Relative wt % of C and R	87:13		54:46		17:83		26:74*		61:39			12:88	—	—
Estimated bulk composition:														
Fe	63·9		60·1		56·9		56·3		59·0‡			—		
Mg	1·4		1·5		1·5		3·4		2·9			—		
Mn	0·6		0·3		0·3		0·7		0·4			—		
Ti	3·5		6·3		7·4		4·5		5·3			5·3		
Al	1·1		1·5		1·6		2·7		1·7			1·5		

Norms of cubic phases:

Grain	7	8	9	10	12 C_1	12 C_2	11
$MgAl_2O_4$	3·0	6·5	13·9	21·9	6·5	24·0	5·3
$MgFe_2O_4$	7·4	7·4	13·4	41·2	19·8	4·0	10·2
$MnFe_2O_4$	2·5	2·1	4·9	8·8	2·8	1·4	1·6
Fe_2TiO_4	11·8	5·6	3·4	1·3	3·5	—	26·7
Fe_3O_4	74·2	77·7	64·3	24·6	67·7	74·2	54·8
Sum	98·9	99·3	99·9	97·8	100·3	103·6‡	98·6

Norms of rhombohedral phases:

Grain	7	8	9	10	12	14
Al_2O_3	0·9	0·2	1·7	1·3	1·1	2·6
$MgTiO_3$	6·0	4·0	5·1	8·2	10·0	5·2
$MnTiO_3$	1·2	0·3	0·3	0·9	0·6	0·9
$FeTiO_3$	23·0	33·6	21·1	8·7	26·4	8·2
Fe_2O_3	68·6	61·2	69·8	81·1	61·1	80·8
Sum	99·7	99·3	98·0	100·2	99·2	97·7

* More than usually intimate intergrowth of cubic and rhombohedral phases adds considerable uncertainty to estimates of their relative proportions and hence to calculation of bulk composition.

† Even the coarser spinel lamellae are too small (1μ wide) to be completely resolved by the 2μ traverse of the electron beam. The calculated normative total of well over 100 % for the spinel (cubic phase 2), even without titanium, strongly suggests that the two major components, iron and titanium, are respectively too high and too low, because of incomplete resolution. The composition of cubic phase 1 includes the finer unresolvable spinel lamellae—that is, they behave in this respect as if they were in solid solution.

‡ Based on cubic phase 1 and the rhombohedral phase.

§ Short 2μ and 5μ step traverses showed no evidence of inh omogeneity and no reason for altering the original identification as a single-phase titanhematite.

must be still richer in $FeTiO_3$, although being narrower, they were less well resolved by the electron beam.

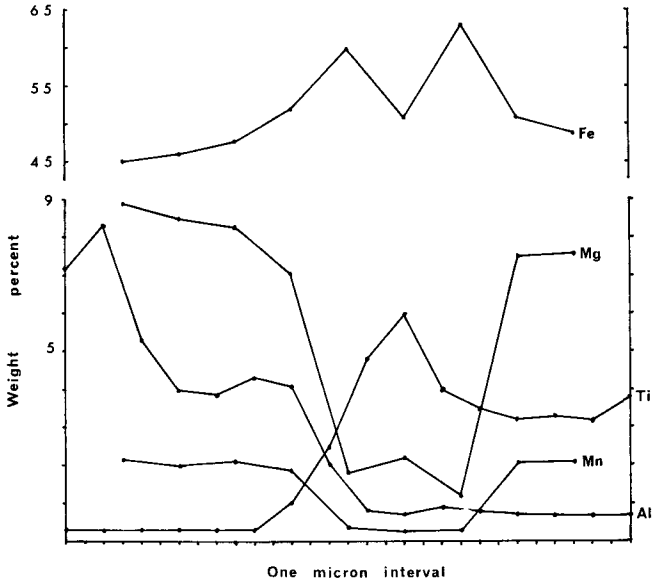

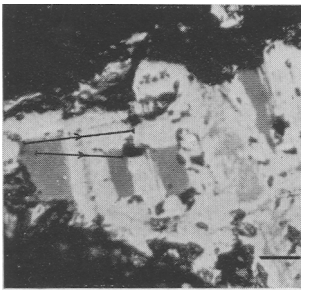

FIG. 6. Grain no. 10 (in ilmenite concentrate, Waikato North Head. No. 9, also fig. 10, of Wright, 1964). Upper traverse on photomicrograph (3μ step): Fe, Mg, Mn. Lower traverse on photomicrograph (2μ step): Ti, Al. Scale bar represents 10μ. *Notes.* Lack of coincidence of peaks at right-hand end of profile due to different traverse paths. Area of X-ray scan pictures (fig. 7) overlaps right-hand part of photomicrograph above.

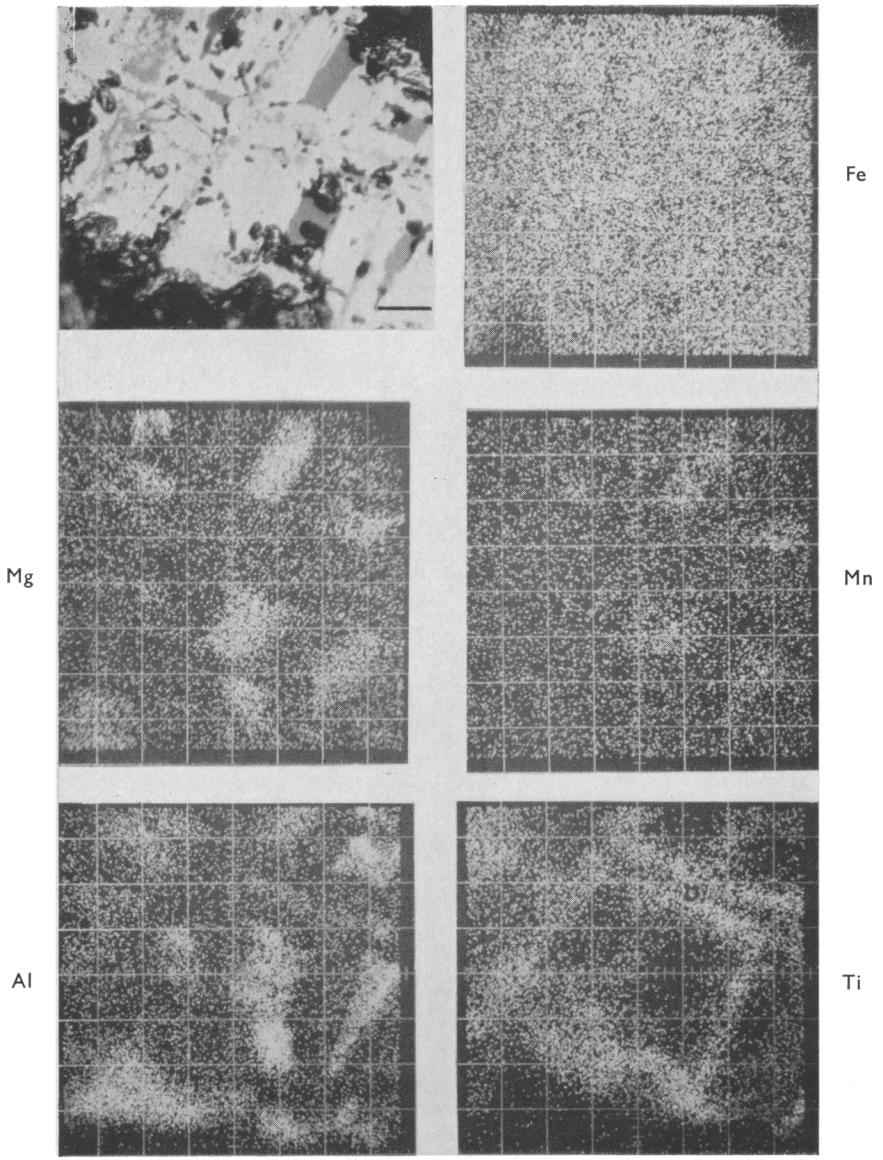

FIG. 7. Grain no. 10. X-ray scan pictures, 10KV excitation potential. Rectangular shape of photomicrograph due to slightly different areas covered by Fe, Mg, Mn pictures on the one hand and by Ti, Al pictures on the other. Scale bar represents 10μ.

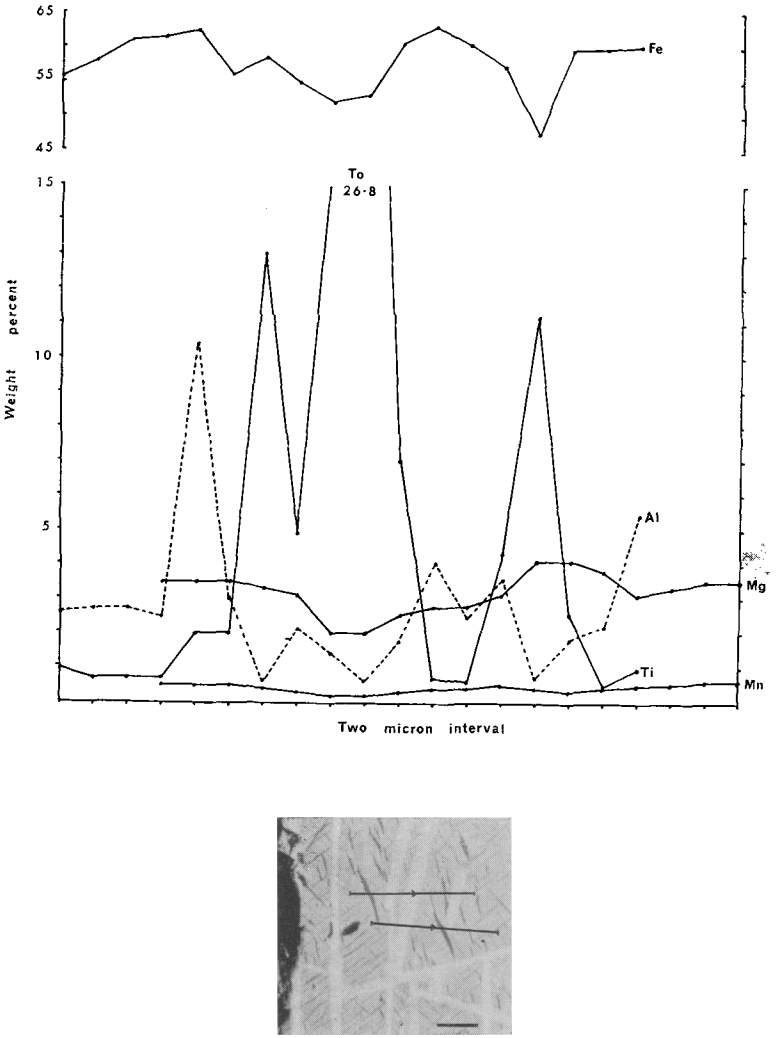

FIG. 8. Grain no. 12 (in titanomagnetite concentrate, Raglan. No. 3 also fig. 3 of Wright, 1964). Upper traverse on photomicrograhh (2μ steps): Fe, Ti, Al. Lower traverse on photomicrograph (2μ steps): Mg, Mn. Scale bar represents 10μ. *Note.* Profile diagram includes information from four traverses, along different paths and with different beam widths. This accounts for lack of peak correspondence in some places.

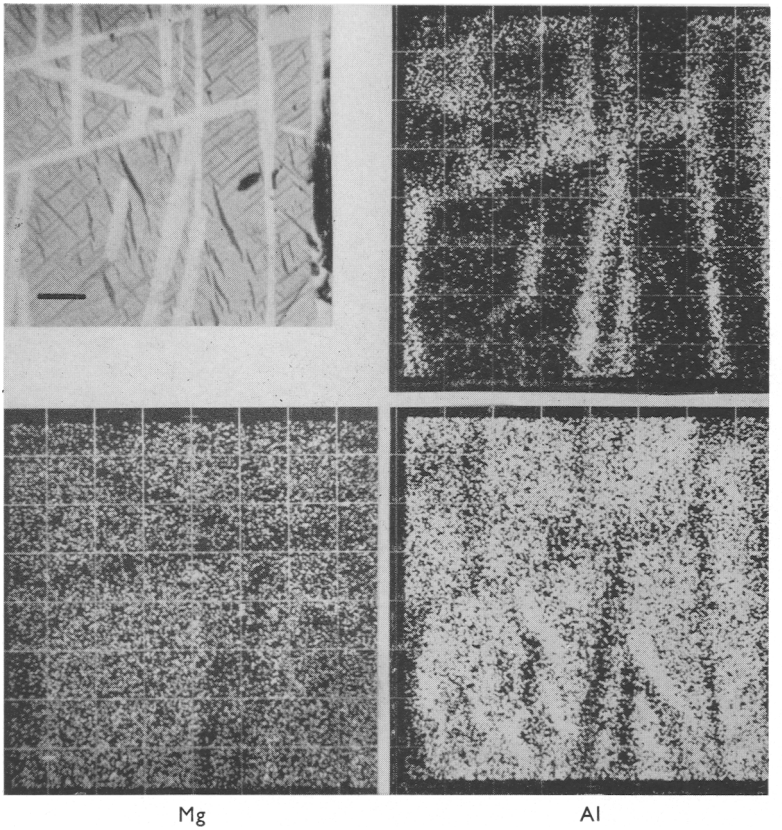

FIG. 9. Grain no. 12. X-ray scan pictures, 10KV excitation potential. Scale bar represents 10μ.

In grain no. 12 the rhombohedral lamellae are wide enough to be fully resolved, so that compositional variations can be attributed to non-equilibrium conditions. The range of Ti contents, from 6 % to 26 %, is particularly striking. Changes of oxygen fugacity in the rapidly cooling volcanic environment could well have been too rapid for equilibrium to be continuously maintained, especially in the early stages when greater migration of titanium was necessary.

Analysed compositions of coexisting cubic and rhombohedral phases lie outside the range of equilibrium compositions presented in Buddington and Lindsley (1964, fig. 5). Some estimate of the limiting conditions

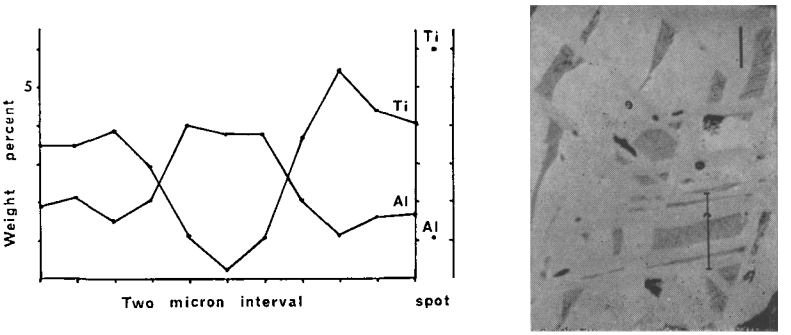

FIG. 10. Grain no. 13 (from titanomagnetite concentrate, Waikato North Head. No. 4, also fig. 9 of Wright, 1964). Traverse on photomicrograph (2μ steps): Ti, Al. Spot in upper middle of photomicrograph also: Ti, Al. Scale bar represents 10μ.

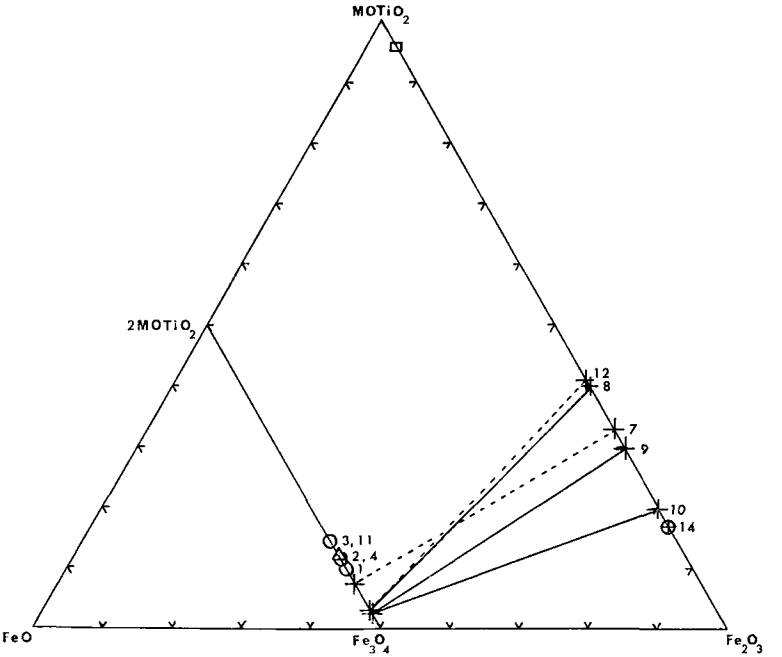

FIG. 11. Compositions of analysed cubic and rhombohedral phases, to show changes on progressive oxidation; molecular percentages. ○, homogeneous titanomagnetites (table I) and grain no. 11, average composition. △, average chemical analysis (table I). +, coexisting cubic and rhombohedral phases in oxidized grains (dotted tie-lines are for grains in which there is doubt whether the analysed rhombohedral phase compositions are representative). ⊕, homogeneous titanhematite. □, ilmenites (table IV).

at commencement of oxidation is possible, however. As discussed above, the ilmenite lamellae in grain no. 7 are unlikely to contain more than 10 % Fe_2O_3, and those in grain no. 11, being considerably greyer, may well carry only about 5 %. The cubic phase contains about 15 % ulvöspinel in grain no. 7, while that in no. 11 can be inferred to contain little more than 20 % (fig. 11). These estimates provide approximate coexisting compositions of $Mt_{85}Usp_{15}$–$Hem_{10}Ilm_{90}$ for grain no. 7, and $Mt_{80}Usp_{20}$–Hem_5Ilm_{95} for grain no. 11. From fig. 5 of Buddington and Lindsley (1964) such compositions would be in equilibrium at temperatures and oxygen fugacities of 650° and $10^{-17.7}$ and 665° C and $10^{-18.2}$ respectively, provided the effect of minor constituents could be ignored.

Minor constituents and the transparent spinels. Analysis figures show that aluminium commences to accumulate in the cubic phase soon after the start of oxidation. According to solvus diagrams in Turnock and Eugster (1962), magnetite will accommodate 14 mol % hercynite ($FeAl_2O_4$) in solid solution at 600° C, while hematite will accept only 6 mol % corundum (Al_2O_3) at the same temperature. An ilmenite-rich rhombohedral phase formed by oxidation of a titanomagnetite would accept still less alumina, since $FeTiO_3$ has a larger cell than Fe_2O_3. By contrast, the cubic phase could accommodate more $FeAl_2O_4$ at this stage, because the cell parameter, in this case initially close to that of Fe_3O_4 (Wright, 1964), would be decreased by removal of the ulvöspinel to form ilmenite-rich lamellae.

Magnesium and manganese do not show the same extremes of interphase partitioning as aluminium, especially at earlier stages of oxidation, presumably because $MgTiO_3$ and $MnFe_2O_4$ also substitute easily in magnetite. But with progressive oxidation only Fe_2O_3 is added to the rhombohedral phase, so that magnesium and manganese would concentrate in the cubic phase, substituting as $M^{2+}Fe_2O_4$ and $M^{2+}Al_2O_4$.

Careful re-examination of polished sections revealed that contrary to an earlier statement (Wright, 1964), there are probably no unoxidized grains containing exsolved transparent spinels. In some grains (e.g. no. 11, fig. 12*a*) the disposition of spinels close to rhombohedral lamellae suggests that (in at least some grains) exsolution followed closely on commencement of oxidation, which must therefore have occurred near or below the magnetite–spinel solvus curve. Those grains showing only the early stages of oxidation (e.g. no. 12) might have evolved in a similar manner. Recalculation of the analysis for cubic phase 1 of grain no. 12—considering magnetite and hercynite molecules alone—gave respective proportions of 89:11 weight per cent. Fe_3O_4 and $FeAl_2O_4$. On the solvus

of Turnock and Eugster (1962) this composition corresponds to 600° C, which is probably a minimum, since entry of the smaller magnesium ion into the spinel structure (cf. cubic phase 2 of grain no. 12) would probably raise the solvus temperature.

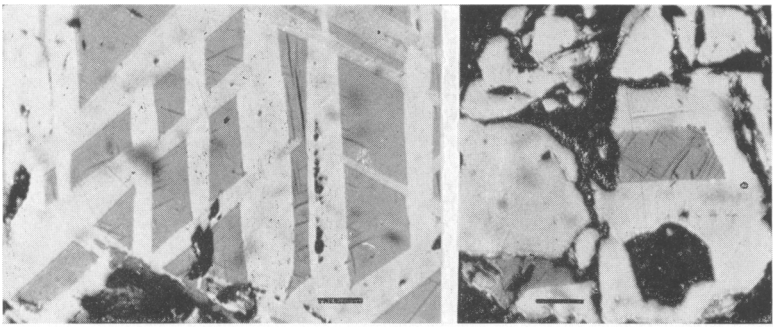

a b

FIG. 12. Oxidized grains with exsolved spinels. Both grains in titanomagnetite concentrate, Raglan. No. 3 of Wright, 1964. Scale bars represent 10μ. (*a*) Spinel lamellae arranged near rhombohedral phase boundaries. This arrangement may represent a more advanced stage of the fine-scale spinels fringing ilmenite lamellae in grain no. 11. (*b*) Spinel lamellae in cubic phase of grain at advanced oxidation stage.

At 550° C and oxygen fugacity of more than 10^{-23}, hercynite solid solutions break down to magnetite–hematite–corundum assemblages (Turnock and Eugster, 1962, fig. 11). But fig. 5 in Buddington and Lindsley (1964) shows that advanced oxidation in these grains must take place under oxygen pressures higher than 10^{-23} at this temperature. This disparity persists to higher temperatures, so that hercynite should break down soon after oxidation commences. It may be that the presence of magnesium in the spinel lamellae (e.g. grain no. 12) inhibits breakdown until much higher oxygen pressures are reached.

Grains showing more advanced stages of oxidation must now be considered:

No. 14. Fully oxidized homogeneous titanhematite, containing little Mg and Al, which presumably were fairly readily accommodated in the Fe_2O_3–$FeTiO_3$ solid solution.

No. 9 (fig. 4). Contains relatively large amounts of Al and Mg in the cubic phase, which contains very sparse spinel lamellae.

Fig. 12*b*. Grain resembling no. 9, but with appreciable exsolved spinels in the cubic phase.

No. 10 (figs. 6 and 7). Contains extremely large amounts of minor constituents in the homogeneous cubic phase.

No. 13 (fig. 10) (incomplete analysis). With less Al (and presumably less Mg) in the cubic phase than either of the previous two, yet crowded with transparent lamellae in the cubic phase.

Whether or not transparent spinels exsolve must depend primarily on the cooling history rather than on composition. But it cannot be established at what stage exsolution of spinels commenced: thus grain no. 12 and the one shown in fig. 12*b* have approximately similar spinel concentrations in the cubic phase. Did the lamellae in the latter separate and start growing when oxidation started, and if so, what would happen to those lamellae in grains like no. 12, crowded with spinel lamellae at an early oxidation stage? To answer such questions, further work must concentrate on examination of these minerals in their original environment.

Correlation of thermomagnetic properties with analyses

Following Vincent *et al.* (1957), the magnetic properties of homogeneous cubic phases in ironsand grains are attributed to their limiting Fe_3O_4 contents. Grains with homogeneous cubic phases are listed in table III, with their limiting Fe_3O_4 contents and corresponding Curie points, determined by using the curves of Chevallier (Vincent *et al.*, 1957). Upon progressive oxidation there is first a rise in Curie points, as early migration of titanium into the rhombohedral phase leaves an iron-enriched cubic phase not yet diluted by significant amounts of minor constituents. As the latter increase in amount, the Curie point must fall again till it is at or below room temperature—which accounts for the presence of grains of this type in the non-magnetic ilmenite concentrates.

TABLE III. Curie points of Cubic Phases

Grain No.	Limiting Fe_3O_4 wt %	Curie point
1 to 4	72 (av.)	405° C
7	85	500
8	88	520
9	71	400
10	27	*c.* – 20

The thermomagnetic curves for magnetic ironsand concentrates have their steepest slope in the vicinity of 400° C, but start their downward curve at about 200° and terminate at a little over 500° (Wright, 1964).

Table III shows that the bulk of the grains (which are homogeneous) should have Curie points in the 400° C range and that the higher Curie points are probably due to the small proportion of grains in early stages of oxidation, while lower ones can be attributed to a few grains near the end of the oxidation process.

The thermomagnetic curves are therefore not indicative of significant variations in bulk composition. They merely indicate the range of cubic phase compositions that are produced by progressive oxidation of original ulvöspinel–magnetite solid solutions covering a relatively small bulk compositional range.

Ilmenites

Two grains in an ilmenite concentrate from Muriwai (no. 8 of Wright, 1964) were analysed and found to be identical in composition, within the limits of accuracy of the method (table IV). The molecular composition of this ilmenite has been plotted on fig. 11. According to fig. 5 in Buddington and Lindsley (1964) such ilmenites could co-exist in equilibrium with titanomagnetite of a composition represented by an average of table I, at about 680° C and oxygen fugacity of 10^{-17}.

TABLE IV. Ilmenite Composition

Fe	34·5	Al_2O_3	—
Mg	1·0	$MgTiO_3$	5·2
Mn	0·5	$MnTiO_3$	1·2
Ti	30·6	$FeTiO_3$	89·2
Al	—	Fe_2O_3	4·8
			100·4

Magnetic concentrate from the west coast of South Island

Partial analysis for Fe, Ti, Mg were made for two magnetite grains in a magnetic concentrate from Gillespies Beach (no. 6 of Wright, 1964), where the iron oxide minerals are derived from metamorphic rocks. An average Fe figure of 72·5 % was obtained, in good agreement with that for pure Fe_3O_4. No titanium or magnesium was recorded and it is possible that the small amount of titanium appearing in the chemical analyses (e.g. Wright, 1964) is due to admixed grains of ilmenite-bearing hematite.

Acknowledgements. Prof. D. S. Coombs kindly read the manuscript and Mr. B. R. Paterson assisted with the illustrations. A research grant from the New Zealand University Grants Committee to defray travel and subsistence costs for one of us (J. B. W.) is gratefully acknowledged.

References

BIRKS (L. S.), 1963. Electron probe microanalysis. Interscience, New York: 253.
BUDDINGTON (A. F.) and LINDSLEY (D. H.), 1964. Journ. Petrology, vol. 5, pp. 310–57.
LOVERING (J. F.) and WHITE (A. J. R.), 1964. *Ibid.*, pp. 195–218.
TURNOCK (A. C.) and EUGSTER (H. P.), 1962. *Ibid.*, vol. 3, pp. 533–65.
VINCENT (E. A.), WRIGHT (J. R.), CHEVALLIER (R.), and MATHIEU (S.), 1957. Min. Mag., vol. 31, pp. 624–55.
WRIGHT (J. B.), 1964. New Zealand Journ. Geol. Geophys., vol. 7, pp. 424–44.
WRIGHT (J. B.), 1965. *Ibid.*, vol. 8, p. 158.

[*Manuscript received 8 July 1965*]